



OPEN Enhancing energy conversion efficiency of electromagnetic repulsion mechanisms through resistance coefficient optimization model

Puyi Cui^{1,2}✉, Guoli Li^{3,4} & Qian Zhang^{1,3}

This study investigates methods to enhance the energy conversion efficiency of electromagnetic repulsion mechanisms. Initially, a model considering the influence of the resistance coefficient on electromagnetic repulsion mechanisms is developed based on electromagnetic principles. Sensitivity analysis of the resistance coefficient is conducted to elucidate its role in energy conversion efficiency. Subsequently, finite element analysis techniques are applied to simulate electromagnetic repulsion mechanisms across varying resistance coefficients to determine the optimal value. Experimental validation of theoretical models and numerical simulation results is then performed, with precise adjustments made to the resistance coefficient during experiments, and energy conversion efficiency accurately measured under diverse conditions. The results indicate a significant improvement in energy conversion efficiency following resistance coefficient optimization. Numerical simulations reveal that setting the resistance coefficient to 0.85Ω yields optimal energy conversion efficiency, with a 23.5% enhancement over the pre-optimized state. Experimental validation corroborates these findings, demonstrating an average 22% increase in energy conversion efficiency compared to the unoptimized state. Comparative analysis with related studies demonstrates an average improvement of 23.5% in energy conversion efficiency, with the maximum enhancement reaching 25.0%. This underscores the effectiveness and superiority of the proposed optimization model. This discovery offers new avenues for designing and enhancing electromagnetic repulsion mechanisms and presents opportunities for improving energy efficiency and performance in associated applications.

Keywords Electromagnetic repulsion mechanism, Energy conversion efficiency, Resistance coefficient optimization model, Finite element analysis

In the technological wave of the 21st century, electromagnetic technology has emerged as a key driver of innovation and development across numerous fields due to its unique advantages and extensive application prospects^{1–3}. As an integral component of electromagnetic technology, the electromagnetic repulsion mechanism operates based on electromagnetic force principles, utilizing current flow in conductors to generate magnetic fields for force conversion and transmission^{4,5}. Renowned for its rapid response, high control precision, and non-contact nature, this mechanism holds vast potential for applications in precision positioning, power transmission, and vibration control^{6,7}. Electromagnetic repulsion mechanisms are extensively utilized in electrical devices such as circuit breakers, relays, and solenoid valves, which are integral to power systems and automation control. In these applications, optimizing electromagnetic repulsion mechanisms enhances equipment performance, reduces energy consumption, and significantly improves the overall reliability and cost-effectiveness of the system.

However, despite these advantages, as technology advances and equipment performance demands increase, the limitations of electromagnetic repulsion mechanisms in energy conversion efficiency have become increasingly

¹School of Electrical Engineering and Automation, Anhui University, Hefei 230601, China. ²Engineering Research Center of Power Quality, Ministry of Education Anhui University, Hefei 230601, China. ³Anhui Key Laboratory of Industrial Energy-Saving and Safety, Anhui University, Hefei 230601, China. ⁴Anhui Collaborative Innovation Center of Industrial Energy-Saving and Power Quality Control Anhui University, Hefei 230601, China. ✉email: virtuosocpi@163.com

evident⁸. Low energy conversion efficiency results in energy wastage, equipment heating, and reduced lifespan, posing significant constraints on the performance and applicability of electromagnetic repulsion mechanisms^{9–11}. Consequently, enhancing the energy conversion efficiency of electromagnetic repulsion mechanisms has become a focal point for both academic and industrial sectors¹². The efficiency of electromagnetic repulsion mechanisms directly influences the energy consumption and operational costs of devices. The energy conversion efficiency of existing electromagnetic repulsion devices is often impacted by various factors, including resistivity, magnetic field distribution, and material properties. Optimizing these factors to enhance energy conversion efficiency remains a critical challenge.

Current research endeavors aimed at enhancing the energy conversion efficiency of electromagnetic repulsion mechanisms primarily concentrate on optimizing mechanism design, improving material properties, and adjusting operating frequencies¹³. While these methods have shown some progress, they often involve intricate design processes or costly materials, constraining their widespread adoption^{14–16}. In contrast, the significance of the resistance coefficient, as a fundamental physical parameter influencing the distribution of electromagnetic fields and currents, remains underexplored in terms of energy conversion efficiency¹⁷. The resistance coefficient not only dictates energy loss in electromagnetic repulsion mechanisms but also impacts the efficiency and stability of electromagnetic force generation, serving as a critical link between electromagnetic fundamentals and efficiency enhancement^{18–20}. However, due to a lack of comprehensive understanding of the underlying mechanisms and systematic optimization approaches, leveraging the resistance coefficient for efficiency improvement remains underdeveloped²¹. Designing and fine-tuning the electromagnetic repulsion mechanism to accurately control and adjust the resistance coefficient for optimal performance is a challenging task. Ensuring the stability and efficiency of the mechanism under varying conditions is crucial for maintaining the reliability of the equipment.

This study addresses these challenges by constructing a model of the electromagnetic repulsion mechanism, conducting an in-depth analysis of the resistance coefficient's impact on energy conversion efficiency, and proposing an optimized solution. Through systematic analysis and optimization of the design parameters, particularly the resistance coefficient, the study aims to enhance energy conversion efficiency. This approach is expected to reduce energy losses in power systems, lower operating costs, and improve the overall economic performance of the system. Addressing this gap, this study introduces a novel approach by constructing a model of electromagnetic repulsion mechanisms that accounts for the influence of the resistance coefficient and elucidates its impact on energy conversion efficiency through sensitivity analysis. Utilizing finite element analysis (FEA) techniques and experimental validation, the study aims to pinpoint the optimal resistance coefficient value to significantly boost the energy conversion efficiency of electromagnetic repulsion mechanisms. This not only furnishes theoretical guidance and technical support for the efficient design and application of such mechanisms but also unveils new avenues for energy utilization efficiency and comprehensive equipment performance enhancement.

Literature review

The electromagnetic repulsion mechanism, a significant application of electromagnetics, has been extensively studied and applied across various domains, including precision manufacturing, robotics, and aerospace. Regarding energy conversion efficiency, numerous research outcomes have been generated by the academic community. Cao et al. (2019)²² optimized the mechanism's structure, resulting in a slight increase in energy conversion efficiency, highlighting the importance of structural design in efficiency enhancement. Sun et al. (2023)²³ investigated ultra-low-frequency vibration energy harvesters and discussed principle-based structural optimization and transducer performance improvement methods. Lv et al. (2022)²⁴ concentrated on novel materials' application, effectively reducing energy loss by utilizing materials with high conductivity and low magnetic hysteresis loss. Additionally, Wang et al. (2023)²⁵ explored the impact of operating frequency on electromagnetic repulsion mechanism efficiency, revealing that appropriate frequency adjustments could enhance energy conversion efficiency to some extent. Liu et al. (2023)²⁶ analyzed the effect of laser heat sources across a wide power range, adjusting the transmission frequency accordingly. Ding et al. (2023)²⁷ examined the "coil-disc" electromagnetic repulsion mechanism, utilizing finite element simulation to optimize structural strength and driving performance. They concluded that reinforcing structural strength and increasing total displacement improved the mechanism's driving performance, providing suitable mechanical parameters for rapid mechanical switch opening and closing requirements. Li et al. (2023)²⁸ compared heat transfer characteristics under various conditions, including single-phase counterflow, subcooled boiling, and saturated boiling, in both rolling and vertical configurations.

While prior studies have advanced the energy conversion efficiency of electromagnetic repulsion mechanisms, limitations persist. Primarily, most research concentrates on mechanism design, material selection, or operating frequency adjustments, neglecting the fundamental electrical parameter: the resistance coefficient^{29–31}. This coefficient directly impacts energy loss in electromagnetic repulsion mechanisms, yet its optimization methods and impact on energy conversion efficiency remain understudied.

To address these gaps, this study proposes a novel approach. Initially, a model of the electromagnetic repulsion mechanism is developed considering the resistance coefficient's influence, integrating electromagnetic theory with resistance coefficient effects on energy conversion efficiency. Next, through systematic sensitivity analysis and resistance coefficient optimization, the study pinpoints its optimal value, offering a fresh avenue for enhancing energy conversion efficiency. Furthermore, employing a hybrid approach of FEA and experimental validation allows for theoretical and numerical model verification, ensuring the optimization model's effectiveness. Through this comprehensive investigation, a deeper understanding of the resistance coefficient's impact mechanism is achieved, paving the way for improved energy efficiency and performance in electromagnetic repulsion mechanisms and related domains, bridging existing research gaps.

Research methodology

Construction of electromagnetic repulsion mechanism model and introduction of resistance coefficient

This study aims to construct an electromagnetic repulsion mechanism model to investigate thoroughly the impact of the resistance coefficient on electromagnetic repulsion effects and energy conversion efficiency. In this study, the focus is on an electromagnetic repulsion mechanism composed primarily of the following components: the excitation coil, which serves as the core component of the system, generates a magnetic field through the current flowing through it. The strength and direction of this magnetic field directly influence the movement of the repulsion disk. The repulsion disk, a passive component, is affected by the magnetic field generated by the excitation coil. Its positional changes reflect the effect of the electromagnetic repulsion force and drive the mechanical system to complete predetermined tasks. The resistance coefficient, which refers to the degree of resistance to the flow of current within the system, is typically represented by resistors or other resistive elements in the circuit. In the context of the electromagnetic repulsion mechanism, the resistance coefficient is defined by Eq. (1):

$$R = \frac{V}{I} \quad (1)$$

In Eq. (1), R denotes the resistance value (resistance coefficient), V signifies the voltage, and I refers to the current. This section outlines the model construction process, highlighting the significance of the resistance coefficient and its incorporation into the model. The electromagnetic repulsion mechanism's essence lies in electromagnetics' fundamental principles, wherein approaching conductors carrying currents generate interaction forces. According to classical electromagnetic theory, when two parallel infinitely long conductors, separated by a distance d , passing currents I_1 and I_2 , respectively, the repulsive force F between them is expressed by Ampere's force law as Eq. (2):

$$F = \frac{\mu_0 \cdot I_1 \cdot I_2}{2\pi \cdot d} \quad (2)$$

In Eq. (2), μ_0 denotes the magnetic permeability in vacuum, a constant.

When constructing the electromagnetic repulsion mechanism model in this study, two parallel electromagnetic coils are arranged, and the distance d between them is adjusted to simulate various electromagnetic repulsion scenarios. This setup enables precise control and measurement of electromagnetic repulsion generated at specific current intensities. To accurately replicate real-world conditions, incorporating the resistance coefficient became essential, as it directly influences current flow, thus impacting the magnitude of electromagnetic repulsion. Hence, the constructed electromagnetic repulsion mechanism model integrates theory with experimentation to simulate and analyze electromagnetic repulsion behavior under specific conditions and its effect on energy conversion efficiency. The model primarily comprises excitation coils (electromagnetic coils) and repulsion discs (metal discs), which generate repulsive forces through electromagnetic interaction. The excitation coil generates a magnetic field upon current application, while the repulsion disc produces electromagnetic repulsion due to the magnetic field's action. This force drives mechanical motion, such as the opening and closing operations of circuit breakers. The resistance coefficient is pivotal in the model, restricting current flow and influencing the excitation coil's magnetic field intensity, thereby adjusting electromagnetic repulsion magnitude. Selecting and adjusting the resistance coefficient are crucial strategies for optimizing energy conversion efficiency.

Illustrated by the opening operation, when disconnecting the circuit, the model applies a pulse current to the excitation coil for a specific duration. This current induces eddy currents in the repulsion disc, generating a magnetic field opposing the excitation coil's current. Consequently, electromagnetic repulsion propels the repulsion disc, initiating mechanical movement in the connected structure (e.g., the moving contact of a circuit breaker) to effectuate the opening action. To provide a clear depiction of the experimental setup, Fig. 1 presents the overall layout of the electromagnetic repulsion mechanism along with its operating principle.

In Fig. 1, the excitation coil remains stationary, while the repulsion disc, linked to the moving contact in the vacuum interrupter chamber via an insulated connecting rod, moves. Initially positioned in proximity (i.e., closed position), during the opening operation, a brief pulse current from the energy storage capacitor drives the repulsion disc via electromagnetic repulsion, thereby mobilizing the connecting rod and the moving contact to accomplish the opening task. The vacuum within the vacuum chamber is maintained through the use of an efficient vacuum pump system in conjunction with advanced sealing technology. The system utilizes a combination of a molecular pump and a mechanical pump. Initially, a mechanical pump, such as a rotary vane pump, is employed for preliminary evacuation, reducing the chamber's pressure to a level suitable for the molecular pump's optimal operation. Subsequently, the molecular pump, typically a turbomolecular pump, continues to evacuate the remaining gas, achieving a high-vacuum state. This combination of pump systems effectively reduces the pressure in the vacuum chamber to the desired level.

To ensure the stability of the vacuum state, gas leak detection equipment, including mass flow meters and helium leak detectors, was employed during the experiment. These devices continuously monitor pressure changes within the chamber to prevent gas leakage and maintain a stable vacuum environment. The vacuum chamber itself is constructed from high-quality stainless steel and is equipped with high-efficiency sealing materials, such as fluororubber seals, to minimize the risk of gas leakage. The target pressure set for the vacuum chamber is 1×10^{-6} mbar, a level classified as high vacuum, which guarantees the stability of the experimental conditions and the reliability of the data. A precise vacuum control system is used to adjust and monitor the chamber's pressure, ensuring that the experimental environment consistently meets the required specifications.

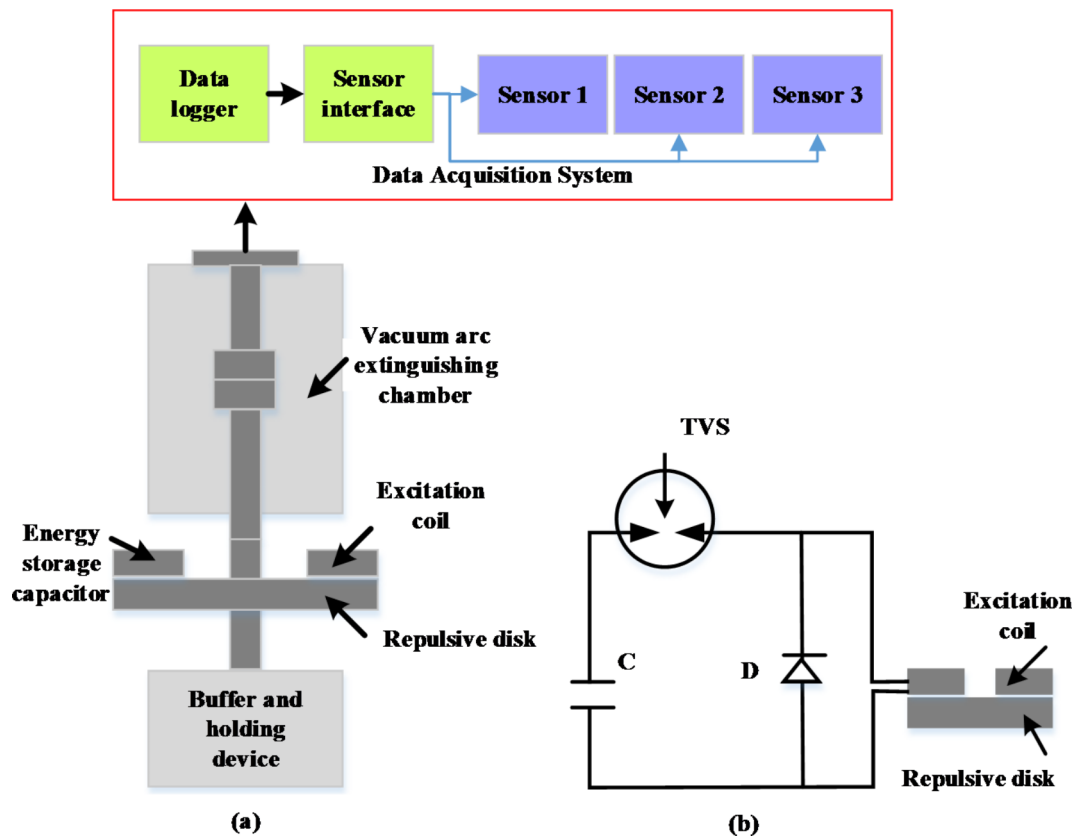


Fig. 1. Overall topology of the electromagnetic repulsion mechanism and its operating principle (a. Overall topology; b. Discharge circuit).

To attain precise control over the resistance coefficient in the electromagnetic repulsion mechanism, this study proposes the utilization of Pulse Width Modulation (PWM) speed control method. By adjusting the duty cycle of the PWM signal, this method indirectly governs the average current flowing through the excitation coil, thereby accurately regulating the electromagnetic repulsion generated. At the core of this design lies a microcontroller-controlled PWM circuit. We opted for a high-performance microcontroller (Arduino) with built-in PWM output functionality as the control core. This microcontroller accepts input commands for resistance coefficient adjustment through its programming interface and modifies the duty cycle of the PWM signal accordingly to regulate the current flowing through the excitation coil.

To transform the PWM signal from the microcontroller into a current with sufficient intensity to drive the excitation coil, we selected a power drive module suitable for high current and high voltage operating conditions. This module, based on Metal-Oxide-Semiconductor Field-Effect Transistor (MOSFET) technology, can adjust the output current based on the duty cycle of the PWM signal. The choice of the drive module takes into account the system's current requirements and heat dissipation performance, ensuring stability and reliability during continuous operation. The PWM control circuit integrates with the selected power drive module into the power supply circuit of the excitation coil, offering an efficient and adjustable current supply system for achieving precise control of the resistance coefficient in the electromagnetic repulsion mechanism. The circuit diagram is depicted in Fig. 2.

In Fig. 2, the microcontroller acts as the central processing unit of the system, generating the PWM signal. The duty cycle of this signal, representing the proportion of time the signal remains high within one cycle, is adjustable to regulate the current intensity flowing through the excitation coil. The PWM control circuit section processes the microcontroller-generated PWM signal to ensure effective driving of the subsequent power drive module. Serving as a signal regulator and amplifier, it maintains the stability and reliability of the PWM signal when handling high currents. The power drive module adjusts the current flowing through the excitation coil based on the PWM signal's duty cycle. MOSFET, a commonly employed high-power semiconductor switch, can handle currents ranging from tens to hundreds of amperes, making it suitable for the electromagnetic repulsion mechanism in this study. The excitation coil directly produces electromagnetic repulsion. By fine-tuning the current in the coil, the magnitude of the repulsive force generated can be precisely controlled, thereby adjusting the influence of the resistance coefficient on the system's performance.

Sensitivity analysis of resistivity coefficient

In the electromagnetic repulsion mechanism, the drag coefficient (or resistivity) plays a critical role in controlling energy loss. The energy conversion efficiency of the mechanism is influenced by the current in the excitation coil,

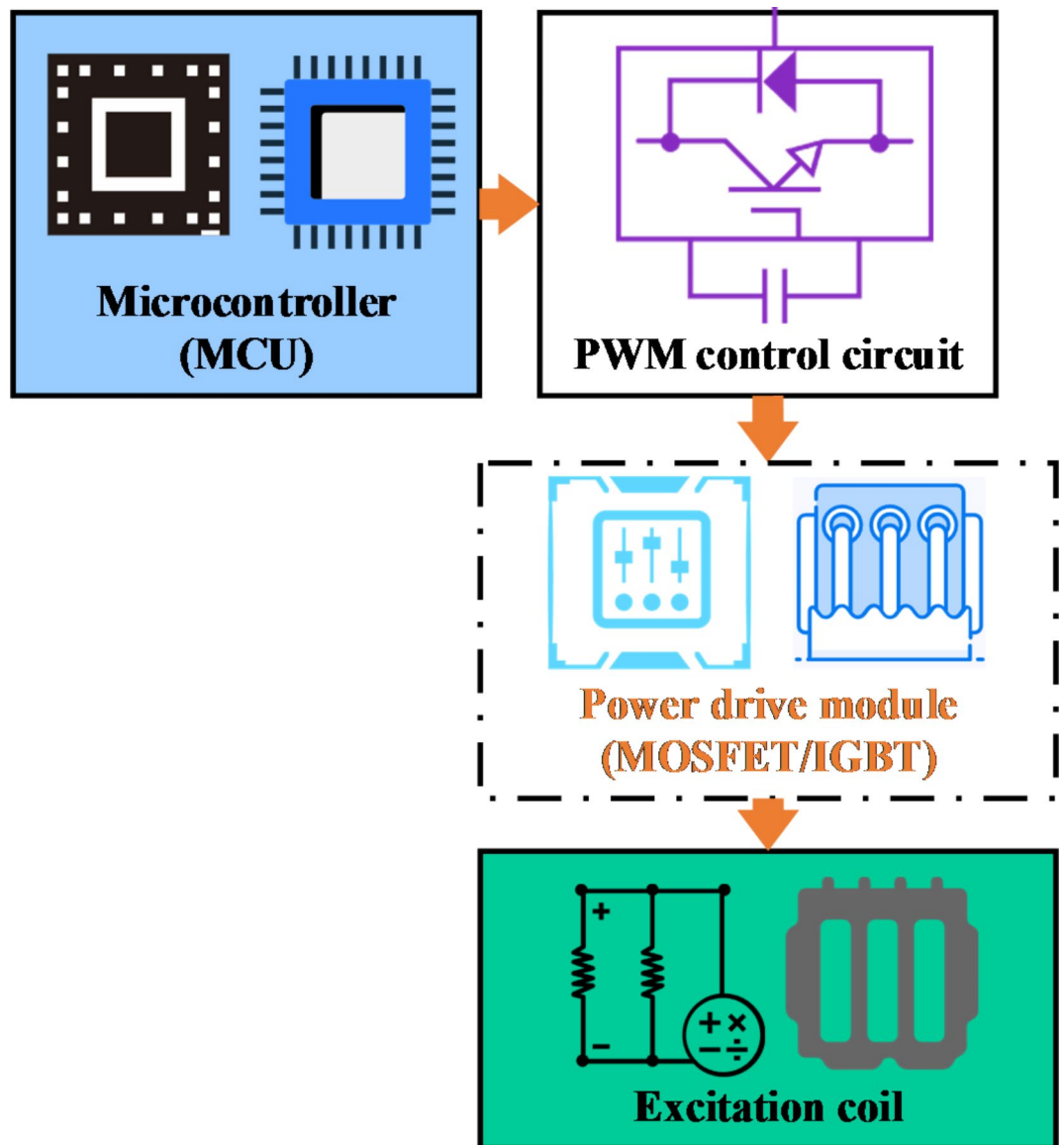


Fig. 2. Integrated structure of PWM control and excitation coil circuit.

which is, in turn, determined by the system's total resistance. Consequently, the drag coefficient directly impacts the magnetic field strength and electromagnetic repulsion force generated by the excitation coil, thereby affecting overall energy conversion efficiency. An increase in the drag coefficient leads to a reduction in current, which weakens the magnetic field strength generated by the excitation coil and results in a diminished electromagnetic repulsion force. This reduction can cause a decline in energy conversion efficiency. Therefore, precise adjustment of the drag coefficient is essential for optimizing the system's energy conversion efficiency.

The electromagnetic repulsion mechanism depends on the flow of current through the electromagnetic coil, with energy loss primarily occurring due to the resistance encountered as current passes through the conductor. According to Joule's law, this energy loss can be expressed by Eq. (3):

$$P = I^2 R \quad (3)$$

In Eq. (3), P represents power loss (i.e., energy loss), I stands for the current intensity, and R is the resistance. As resistance R increases, so does the energy loss when current flows through the conductor, as heat dissipation caused by resistance reduces the system's overall energy efficiency.

Specifically, when current flows through a material with high resistance, the resistive effect causes the current to be converted into heat within the conductor, leading to energy loss. This loss can be effectively minimized by optimizing the resistivity R . For instance, choosing a conductor material with lower resistance or enhancing the conductor design can significantly reduce energy loss. Such optimization not only boosts the energy conversion efficiency of the electromagnetic repulsion mechanism but also enhances the system's overall performance.

In the relevant literature, researchers have extensively examined the impact of resistivity on energy loss. For instance, Li et al. (2019)³² highlighted that optimizing the resistance characteristics of conductors can substantially enhance the system's energy efficiency. Yin et al. (2023)³³ empirically verified the specific effects of varying resistivity on energy loss, demonstrating that low-resistance materials can reduce energy loss in practical applications, thereby improving the performance of electromagnetic systems.

The energy conversion mechanism explored in this study primarily focuses on the operating principles of electromagnetic repulsion mechanisms. These mechanisms generate a magnetic field by energizing a coil, which subsequently exerts an electromagnetic repulsion force on a repulsion disk. The movement induced by this electromagnetic force drives a mechanical system or executes switching operations. The core of this energy conversion process involves the transformation of electrical energy into mechanical energy, with a focus on optimizing the efficiency of this conversion. The energy conversion process involves several key steps: initially, a change in the current within the excitation coil generates a varying magnetic field. This magnetic field then exerts a repulsion force on the repulsion disk, causing its displacement. The displacement is subsequently converted into mechanical motion to perform specific tasks, such as switching operations. The energy conversion efficiency of the electromagnetic repulsion mechanism is ultimately calculated and evaluated by the ratio of the output mechanical energy to the input electrical energy.

To further investigate the specific influence of the resistance coefficient on energy conversion efficiency in electromagnetic repulsion mechanisms, this study employs a sensitivity analysis approach. This process primarily examines how variations in the resistance coefficient affect energy conversion efficiency, thereby elucidating the extent of its impact on system performance. Initially, the resistance coefficient R is designated as the main variable under study. Energy conversion efficiency η is defined as the ratio of output energy E_{out} to input energy E_{in} :

$$\eta = \frac{E_{out}}{E_{in}} \quad (4)$$

Figure 3 depicts the sensitivity analysis process.

During the implementation of the sensitivity analysis, a benchmark resistance value R_0 is first established as the initial reference point. This benchmark value can be derived from theoretical calculations, previous research, or experimental measurements. For instance, $R_0 = 1\Omega$ may be selected as the initial value to facilitate comparison with other resistance coefficient values. Under this benchmark, the initial energy conversion efficiency η_0 of the system is recorded, providing a baseline for subsequent analysis.

Next, the range of the resistance coefficient is defined. The resistance coefficient R is systematically varied within a range of 0.1Ω to 10Ω . To ensure both comprehensiveness and precision in the analysis, measurements are taken at 0.5Ω intervals. This setting enables the capture of subtle effects that the resistance coefficient may have on system performance. For each selected resistance coefficient value, numerical calculation software, such

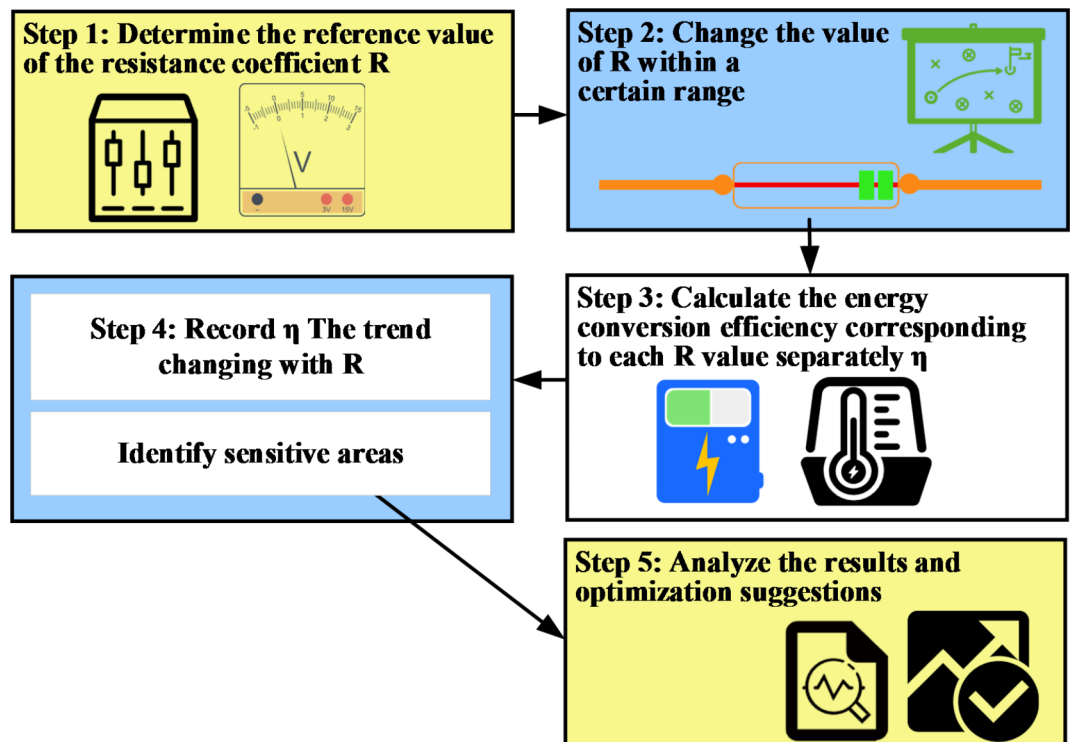


Fig. 3. Sensitivity analysis.

as MATLAB, is employed to compute the corresponding energy conversion efficiency η . These software tools efficiently handle complex computational tasks, delivering accurate results. Once the calculations are completed, the energy conversion efficiency at each resistance coefficient value is meticulously recorded, along with relevant experimental data, including the current and voltage of the excitation coil, the displacement and force of the repulsion disk, and other pertinent parameters.

The relationship between the resistance coefficient R and energy conversion efficiency η is then plotted to analyze how efficiency trends with changes in the resistance coefficient. By examining these plots, intervals where efficiency changes most significantly are identified, highlighting the sensitivity regions. These sensitivity regions indicate the ranges where the resistance coefficient exerts the greatest impact on system performance. Based on the sensitivity analysis results, optimization recommendations are made to guide the selection of the optimal resistance coefficient for achieving the highest energy conversion efficiency. For instance, if the highest efficiency is observed at $2\ \Omega$, it is advisable to focus optimization efforts around this value. Additionally, adjustments to other system parameters, such as current and voltage, are recommended to further enhance overall system performance. The optimization plan includes detailed recommendations for adjustments and anticipated performance improvements.

To verify the accuracy of the sensitivity analysis, experiments are conducted on a practical experimental platform. The resistance coefficient is adjusted to the optimal value suggested by the analysis, and the actual energy conversion efficiency of the system is measured. This verification confirms the validity of the analysis results. Feedback from these experiments lead to adjustments in the analysis model and calculation methods to ensure the accuracy and reliability of the findings.

FEA simulation

This study advances the understanding of electromagnetic repulsion mechanisms by leveraging FEA technology to conduct comprehensive simulations across various resistance coefficient values. ANSYS Maxwell, a leading software for finite element analysis (FEA) in electromagnetic field simulations, is utilized for this study. Renowned for its ability to handle complex electromagnetic problems, ANSYS Maxwell is particularly adept at modeling and analyzing electromagnetic repulsion mechanisms. The software is chosen due to its robust electromagnetic field solving capabilities, advanced mesh generation technology, and comprehensive post-processing functions, which facilitate accurate simulation and detailed performance analysis of electromagnetic repulsion mechanisms. FEA, enabled by ANSYS Maxwell, accommodates the electromagnetic properties of various materials and accurately simulates their responses to electromagnetic fields. This capability allows for precise control over the resistance coefficient in a virtual setting, facilitating a detailed examination of its impact on system performance, notably energy conversion efficiency. The governing equations used in the simulations are as follows:

$$\nabla \cdot D = \rho_f \quad (5)$$

$$\nabla \cdot B = 0 \quad (6)$$

$$\nabla \times E = -\frac{\partial B}{\partial t} \quad (7)$$

$$\nabla \times H = J + \frac{\partial D}{\partial t} \quad (8)$$

Here, D signifies the electric displacement vector, B is the magnetic induction intensity, E is the electric field intensity, H is the magnetic field intensity, J is the current density, and ρ_f is the free charge density. The formulas for calculating the electromagnetic force and magnetic field distribution are employed to further analyze the performance of the electromagnetic repulsion mechanism.

$$F = \int_S (J \times B) \cdot dS \quad (9)$$

The specific steps of the FEA simulation are elucidated in Fig. 4.

Figure 4 illustrates the initial construction of a detailed three-dimensional model, faithfully representing the geometric structure and components of the electromagnetic repulsion mechanism, serving as the simulation groundwork. Subsequently, the model undergoes subdivision into small, computable elements through meshing, ensuring calculation accuracy crucial for reliable results. Electrical current or voltage excitation is then applied to the model, mimicking the generation and fluctuation of the electromagnetic field under real-world conditions.

In the simulation, the electromagnetic coil is represented as a cylindrical structure, with geometric dimensions and current distribution configured to match the actual specifications and operating conditions of the experimental device. The coil is modeled using a conductive material, such as copper, with accurately specified conductivity to replicate real-world working conditions. The repulsion disk is represented as a circular metal disk made from a ferromagnetic material with high magnetic permeability. This material is selected to produce a pronounced magnetic response in the presence of an electromagnetic field, thereby generating a substantial electromagnetic repulsion force. To accurately simulate the vacuum conditions typical of real operating environments, an insulating vacuum cavity is incorporated into the model. The boundary conditions for this vacuum cavity are set to an ideal insulating boundary, allowing the simulation to reflect the effects of the vacuum environment on the electromagnetic field.

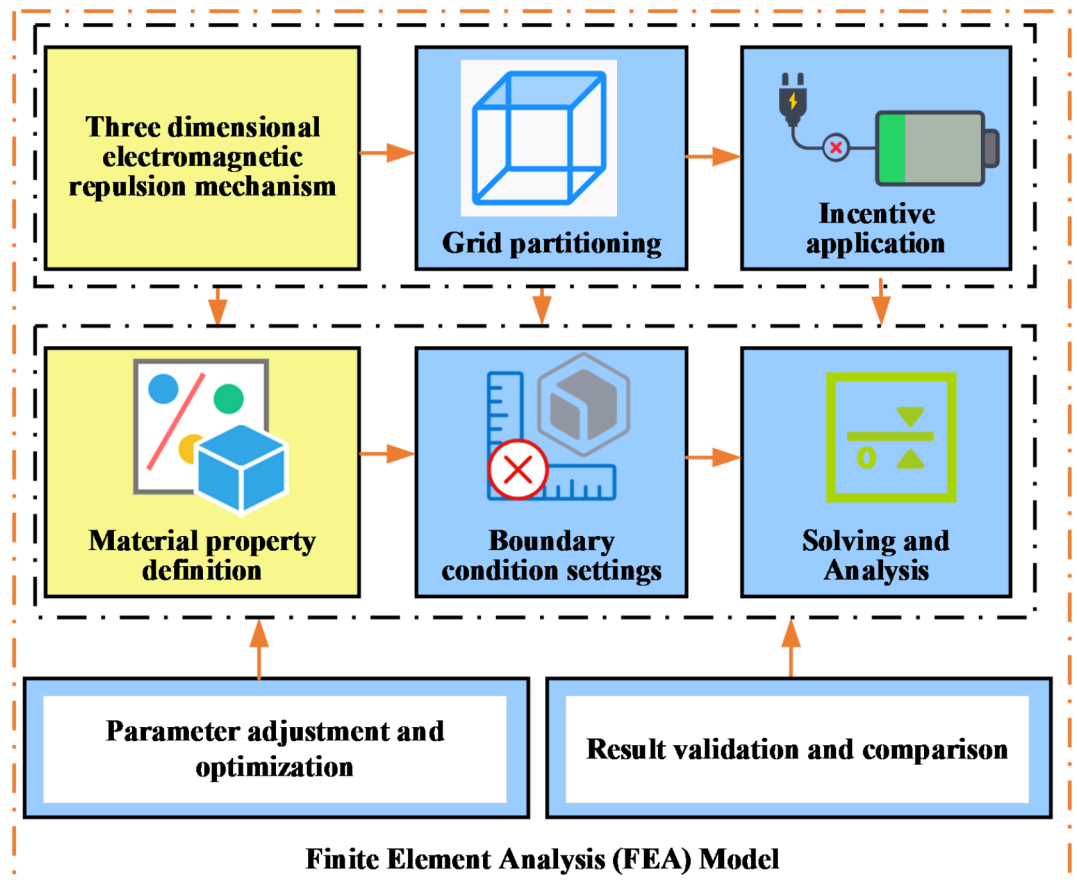


Fig. 4. Process of FEA simulation.

To enhance simulation fidelity, it is imperative to define the electromagnetic properties of each material (such as conductivity, permeability, etc.) and set appropriate boundary conditions governing electromagnetic field behavior. In the interaction region between the electromagnetic coil and the repelling disk, electromagnetic boundary conditions are established to accurately simulate the distribution of current and magnetic fields during operation. The current input to the electromagnetic coil is implemented through a current source boundary condition, while the repelling disk is modeled with a boundary condition representing a ferromagnetic material with constant magnetic permeability to ensure precise electromagnetic field calculations. Magnetic field symmetry conditions are applied at the boundaries of the simulation model, typically setting the normal component of the magnetic field to zero to prevent field penetration through the model's boundaries. The electric potential boundary condition is used to simulate the potential difference between the electrodes, and the tangential component of the electric field is set to zero at the insulating boundaries. Preset current density and potential difference are applied to the contact surface between the electromagnetic coil and the repelling disk to replicate the electromagnetic interaction under real operating conditions.

The meshing strategy employs a combination of tetrahedral and hexahedral meshes. Tetrahedral meshes are utilized for complex geometric structures, such as the electromagnetic coil, to enhance local mesh density. For more regular structures, like the repelling disk, hexahedral meshes are used to maintain overall mesh quality and computational efficiency. In critical areas, particularly where magnetic field gradients change sharply, a higher mesh density is applied to increase computational accuracy. Mesh element sizes in these regions are restricted to within 1 mm to capture subtle variations in the electromagnetic field. The commercial FEA software's automatic mesh generation tool is used, with local mesh refinement applied. A mesh independence test is conducted to confirm that further mesh refinement does not significantly alter the simulation results, ensuring the validity of the mesh configuration.

FEA software is utilized to solve the model, computing essential physical quantities like electromagnetic field distribution and repulsive force generation under specified excitations and conditions. Post-solution, model parameters (e.g., resistance coefficient) are fine-tuned, and multiple simulations are executed to optimize mechanism performance. Ultimately, simulation outcomes are compared against theoretical or experimental data to validate model accuracy and refine it for improved predictive capability.

Experimental platform construction and energy conversion efficiency measurement

Upon completion of the theoretical exploration and simulation analysis, the critical phase of this study involves constructing an experimental platform to ascertain and validate the effect of the resistance coefficient on the

energy conversion efficiency of the electromagnetic repulsion mechanism. The construction of the experimental platform includes assembling several key components: the power supply, resistance adjustment module, excitation coil, repulsion disk, displacement sensor, and force sensor. The power supply provides a stable current source essential for the electromagnetic coil's operation, with precise adjustment of its output voltage and current to ensure data reliability. The resistance adjustment module, comprising a high-precision variable resistor or a specialized resistance adjustment device, allows for fine-tuning of the resistance coefficient within a range of 0.1 Ω to 10 Ω , with step changes of 1 Ω . This fine adjustment is crucial for evaluating the impact of the resistance coefficient on energy conversion efficiency.

The excitation coil, responsible for generating the magnetic field, must be designed and installed to ensure uniform magnetic field distribution, achieving the desired electromagnetic repulsion effect. The repulsion disk, which responds to the magnetic field generated by the coil, has a mass of 500 g with an initial distance set to 5 mm. Displacement and force sensors are employed to measure the displacement and electromagnetic repulsion force of the disk. The displacement sensor must achieve micron-level accuracy, while the force sensor requires calibration to ensure precise measurement. After assembling the experimental device, meticulous installation and calibration of each component are essential for accurate experimental results. The power supply's output voltage and current are verified using calibration equipment. The resistance adjustment module is calibrated to ensure that its resistance settings align with the actual values. Precise alignment of the excitation coil and repulsion disk is necessary to prevent installation deviations from affecting experimental outcomes. Additionally, the displacement and force sensors are calibrated using known standards to guarantee data accuracy.

During the experiment, a high-precision data acquisition system is employed to continuously record the current, voltage, displacement, and force of the excitation coil.

- 1) Current Measurement: A high-precision current sensor is utilized to monitor the current intensity. The data acquisition system recorded the current value at a frequency of 10 Hz to ensure both accuracy and real-time data capture.
- 2) Displacement Measurement: A laser displacement sensor, chosen for its non-contact measurement capabilities, provides high-precision monitoring of the repulsion disk's movement. With a resolution of 0.01 mm, this sensor is able to detect even minute displacement changes.
- 3) Force Measurement: A strain gauge force sensor, characterized by its high sensitivity and stability, is used to measure the electromagnetic repulsion force. The sensor, with a measurement range of 0 to 1000 Newtons and an accuracy of 1%, provides precise force readings.

The data acquisition system comprises a data recorder, sampling module, and computer interface, facilitating real-time monitoring and storage of experimental data. Energy conversion efficiency is determined by the ratio of output energy to input energy. Output energy is calculated based on the repulsion force and displacement, while input energy is derived from the current and voltage of the excitation coil. To ensure result reliability, the experiment is repeated under varying conditions to verify data stability. The experimental setup is controlled for temperature and humidity to minimize environmental effects on measurements. Additionally, the use of a vacuum chamber mitigates air resistance interference. Data from each measurement are averaged and processed to minimize random errors. Table 1 provides the primary parameter settings for the experiment.

Results and discussion
Energy conversion efficiency under theoretical model

Figure 5 presents a comprehensive comparison of theoretical simulated efficiency, elucidating the impact of varying resistance coefficients on energy conversion efficiency and the corresponding enhancement rate relative to the baseline value.

The data depicted in Fig. 5 illustrates a notable upward trend in energy conversion efficiency as the resistance coefficient incrementally rises from 0.6 Ω to 0.85 Ω . During this range, efficiency escalates from 75 to 86%, indicating a positive correlation between the resistance coefficient and energy conversion efficiency up to an optimal point, approximately 0.85 Ω in this investigation. Beyond this optimal threshold, further increases in the resistance coefficient induce a decline in energy conversion efficiency.

Under lower resistance coefficient conditions, elevated circuit currents may lead to heightened energy loss in the electromagnetic repulsion mechanism, primarily in the form of heat, thereby diminishing energy conversion efficiency. Conversely, an increase in the resistance coefficient reduces circuit current, theoretically fostering efficiency. However, surpassing a certain threshold triggers heightened voltage drop across the circuit despite

Parameter category	Parameter name	Setting value
Circuit parameters	Resistivity(ρ)	0.1 Ω – 10 Ω (step 1 Ω)
	Capacitance(C)	1000 μ F
	Current(I)	Measurement range: 0–10 A
Mechanical parameters	Repulsion disk mass (m)	500 g
	Initial distance between repulsion disk and coil (d)	5 mm
Kinetic parameters	Full stroke time	Measurement range: 0–100 ms
Buffer mechanism parameters	Buffer resistance	50 N

Table 1. Parameter settings.

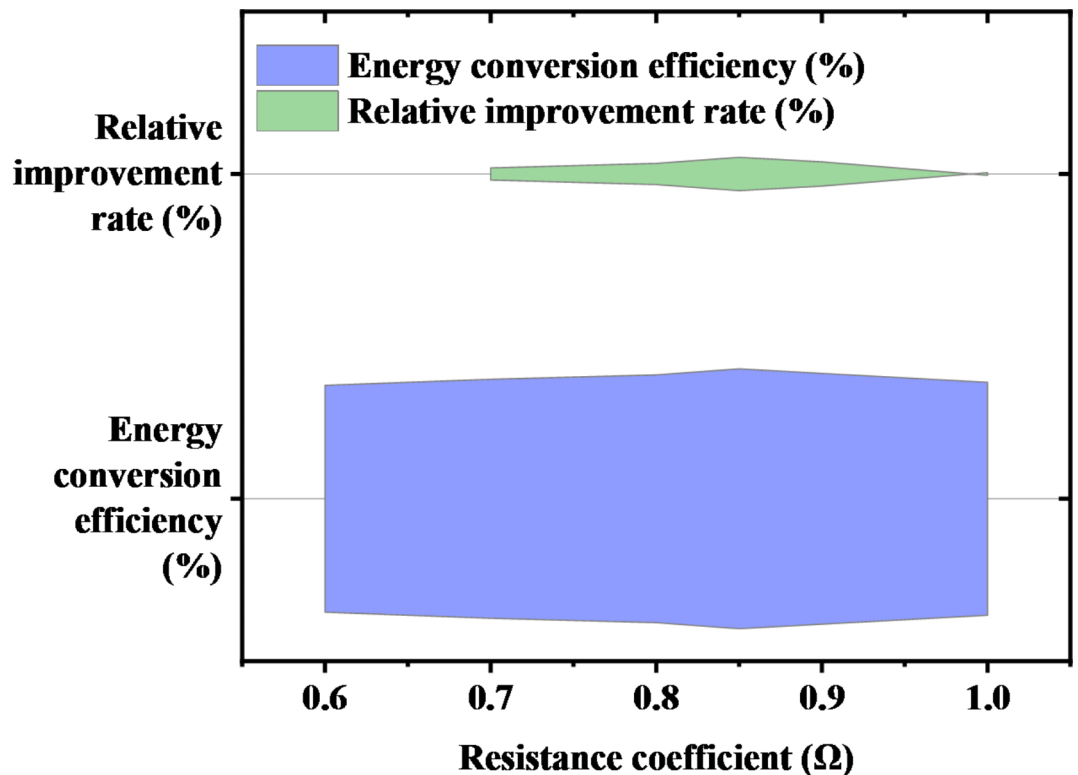


Fig. 5. Comparison of theoretical simulated efficiency under different resistance coefficients.

reduced current. This excessive resistance-induced voltage drop inversely impacts energy conversion efficiency. Consequently, this efficiency-resistance coefficient relationship highlights the existence of an optimal point, approximately 0.85 Ω in this study, maximizing energy conversion efficiency in the electromagnetic repulsion mechanism.

Energy conversion efficiency in experimental platform verification

Figure 6 illustrates the empirical validation of theoretical analysis, showcasing the energy conversion efficiency data under various resistance coefficients on the experimental platform, alongside their corresponding enhancement rates.

The data presented in Fig. 6 corroborates the results of theoretical simulations, providing empirical evidence for the impact of resistance coefficient variation on energy conversion efficiency in the electromagnetic repulsion mechanism. Notably, at a resistance coefficient of 0.85 Ω , the experimental efficiency peaks at 84%, marginally lower than the theoretical prediction of 86%. This slight deviation may arise from practical imperfections such as material defects, internal system losses, and environmental factors. Despite these discrepancies, the experimental outcomes exhibit favorable alignment with theoretical projections, affirming the reliability and validity of the theoretical model in elucidating the significant role of resistance coefficient optimization in enhancing energy conversion efficiency. Table 2 illustrates the impact of input current on energy conversion efficiency.

As depicted in Table 2, the energy conversion efficiency increases with the input current, peaking at 84% when the current is 10 A. This trend indicates that higher currents enhance the energy conversion capacity of the electromagnetic repulsion mechanism, as the increase in current generally intensifies the electromagnetic field, thereby improving system output efficiency. However, beyond 10 A, a slight decrease in efficiency is observed. This reduction may be attributed to several factors: increased resistance and electromagnetic losses due to higher currents lead to greater total energy loss, which can inhibit further efficiency gains. Elevated currents also generate additional heat, potentially causing overheating of electromagnetic components and impacting system performance. Moreover, at high current levels, the magnetic core material may approach saturation, diminishing the potential for further increases in magnetic field strength and efficiency. Therefore, while moderate increases in current can enhance efficiency, a balance between current levels and thermal management is crucial to avoid efficiency degradation from excessive current.

Table 3 provides the energy conversion efficiency of the system at different ambient temperatures.

Table 3 illustrates the impact of ambient temperature on energy conversion efficiency. As ambient temperature rises, the efficiency of the system progressively decreases. This decline can be attributed to several factors: increased temperature typically results in higher resistance of the conductive materials, as elevated thermal energy intensifies electronic movement, leading to greater resistance and increased energy loss, which reduces system efficiency. Additionally, higher temperatures generate more thermal noise, which not only contributes to greater heat loss but may also disrupt the stability of the electromagnetic field, further compromising efficiency.

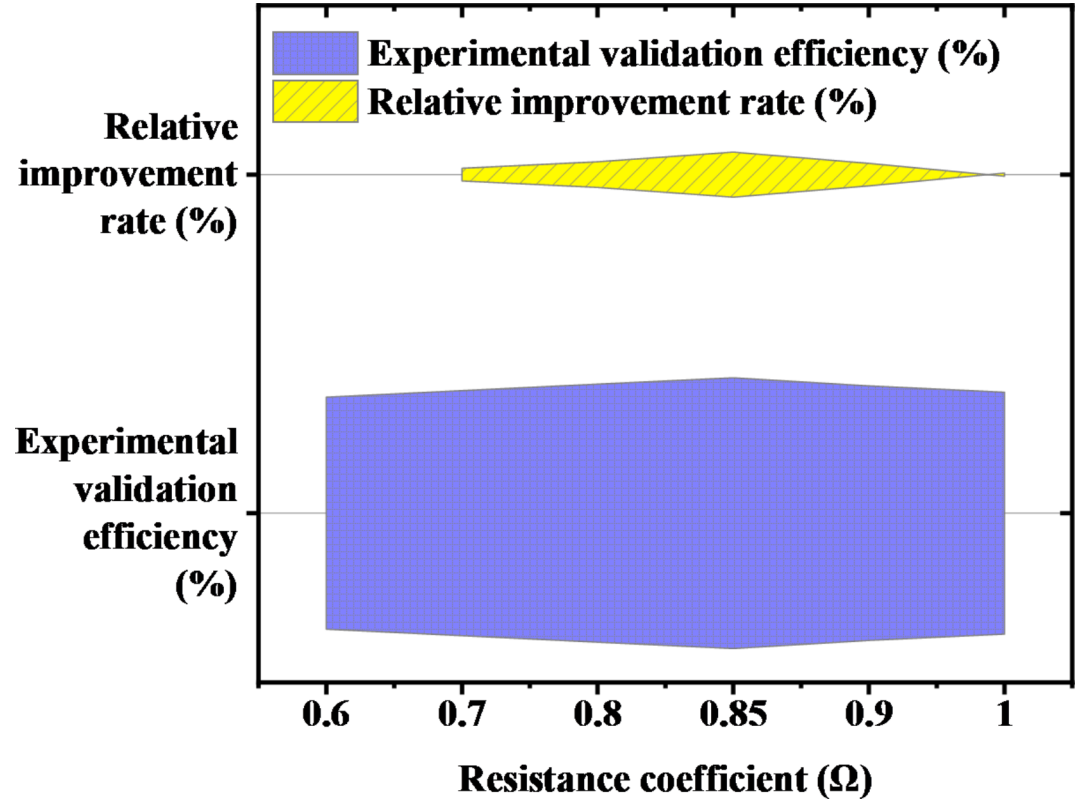


Fig. 6. Energy conversion efficiency data under experimental platform verification.

Input current (A)	Energy conversion efficiency (%)
5	78
6	80
7	82
8	83
9	83.5
10	84
11	83.8
12	82.5

Table 2. Effect of input current on efficiency.

Ambient temperature (°C)	Energy conversion efficiency (%)
25	84
30	83.8
35	83.5
40	83.2
45	82.8
50	82.5

Table 3. Effect of ambient temperature on efficiency.

Conversely, low temperatures may lead to condensation, potentially causing short circuits and affecting overall system stability and efficiency. The data and analysis suggest that both input current and ambient temperature must be carefully managed to optimize the system's energy conversion efficiency. Effective control of these variables in practical applications ensures that the system maintains high performance under varying operational conditions. Figure 7 presents the comparison of discrepancy between theoretical and experimental efficiency.

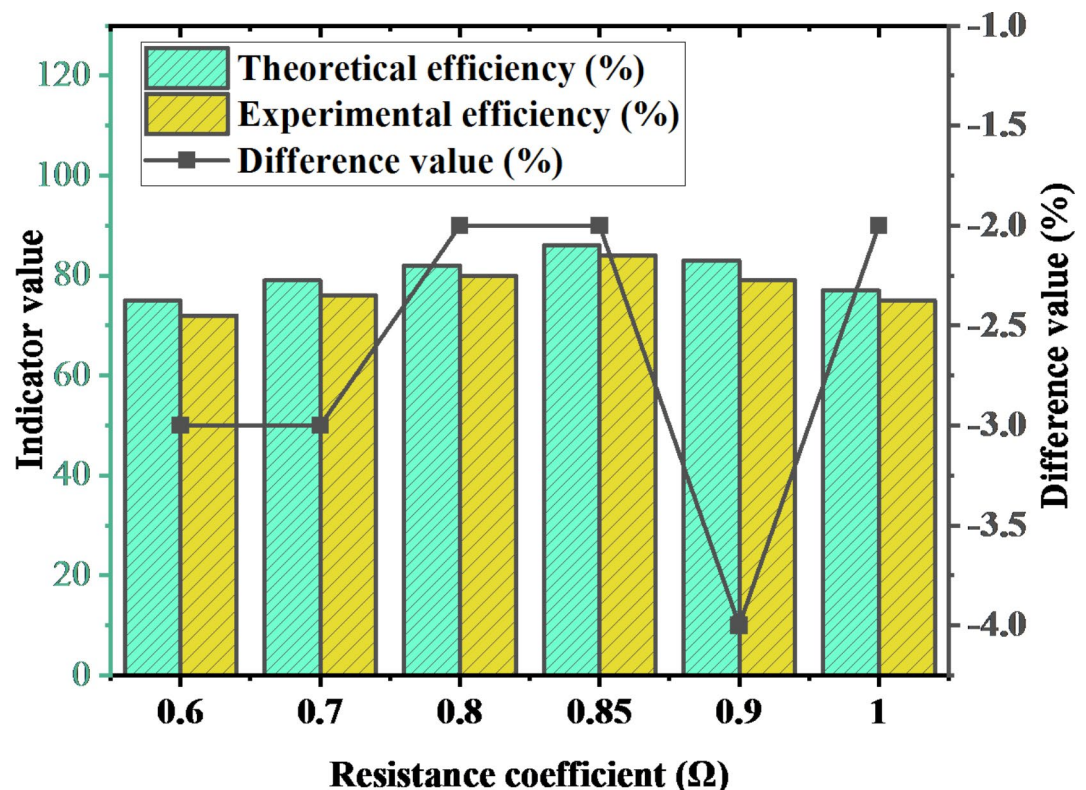


Fig. 7. Comparison of discrepancy between theoretical and experimental efficiency.

The comparison in Fig. 7 reveals generally minor differences between theoretical and experimental efficiencies, with discrepancies not exceeding 4%. This underscores the high reliability and accuracy of both the theoretical model and experimental setup in this study. These variations may arise from random experimental errors, environmental fluctuations, and simplifications inherent in the theoretical model. Notably, at a resistance coefficient of 0.9 Ω , the disparity peaks, suggesting either heightened sensitivity of the system's behavior to resistance coefficient changes or the need for enhanced predictive accuracy in this range. This underscores the importance of conducting a thorough investigation into the relationship between resistance coefficients and system performance, accounting for potential non-ideal factors, to further refine the model's predictive capacity and experimental precision in future research.

Resistivity optimization performance comparison

At the optimized resistance coefficient of 0.85 Ω , Fig. 8 presents a detailed analysis of efficiency enhancement and error comparison. By juxtaposing efficiency improvement and relative errors pre- and post-optimization, we can evaluate the efficacy of the resistance coefficient optimization strategy and ascertain the alignment between theoretical predictions and experimental findings, offering vital insights for further research and applications.

Figure 8 delineates a notable surge in energy conversion efficiency upon adjusting the resistance coefficient to 0.85 Ω . Theoretical simulations demonstrate efficiency soaring from 62 to 86% post-optimization, marking a substantial 24% enhancement. This improvement underscores the pivotal role of the resistance coefficient in dictating energy conversion efficiency. The minimal relative error of $\pm 1.5\%$ underscores the high fidelity between model forecasts and real-world outcomes, underscoring the precision and reliability of the model. During experimental validation, efficiency escalates from 65 to 84% post-optimization, reflecting a 19% enhancement, marginally lower than theoretical predictions but affirming the efficacy of resistance coefficient optimization in augmenting efficiency. The slight relative error of $\pm 1.2\%$ further underscores the robustness and accuracy of the experimental findings.

Figure 9 provides a comparative analysis of efficiency enhancements achieved through resistance coefficient optimization in this study against similar alternative technological approaches, offering a comprehensive perspective on efficiency enhancement strategies. The improvement in efficiency is determined through experimental measurements and simulation analysis of energy conversion efficiency across varying drag coefficient settings. The enhancement is quantified by comparing the energy conversion efficiency before and after optimization. Additionally, a comparison with efficiency data from three related studies is conducted to validate the relative advantages of the proposed method. Among the studies compared, Study A³⁴ delves into materials science, aiming to boost the performance of electromagnetic repulsion mechanisms by optimizing materials. It explores the utilization of highly conductive or high-permeability materials to augment energy conversion efficiency. Study B³⁵ focuses on structural design, striving for efficiency optimization by adjusting the shape, size, or arrangement of mechanisms. It aims to achieve optimal energy conversion performance

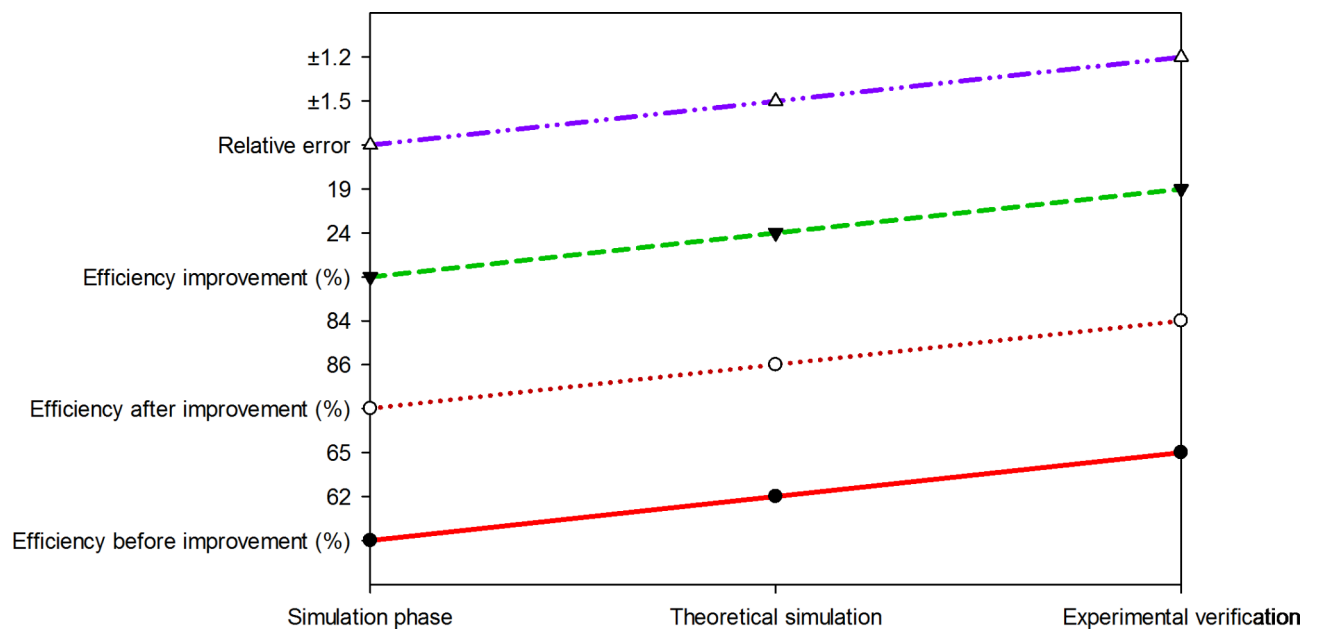


Fig. 8. Efficiency improvement and error comparison at the resistance coefficient of 0.85Ω .

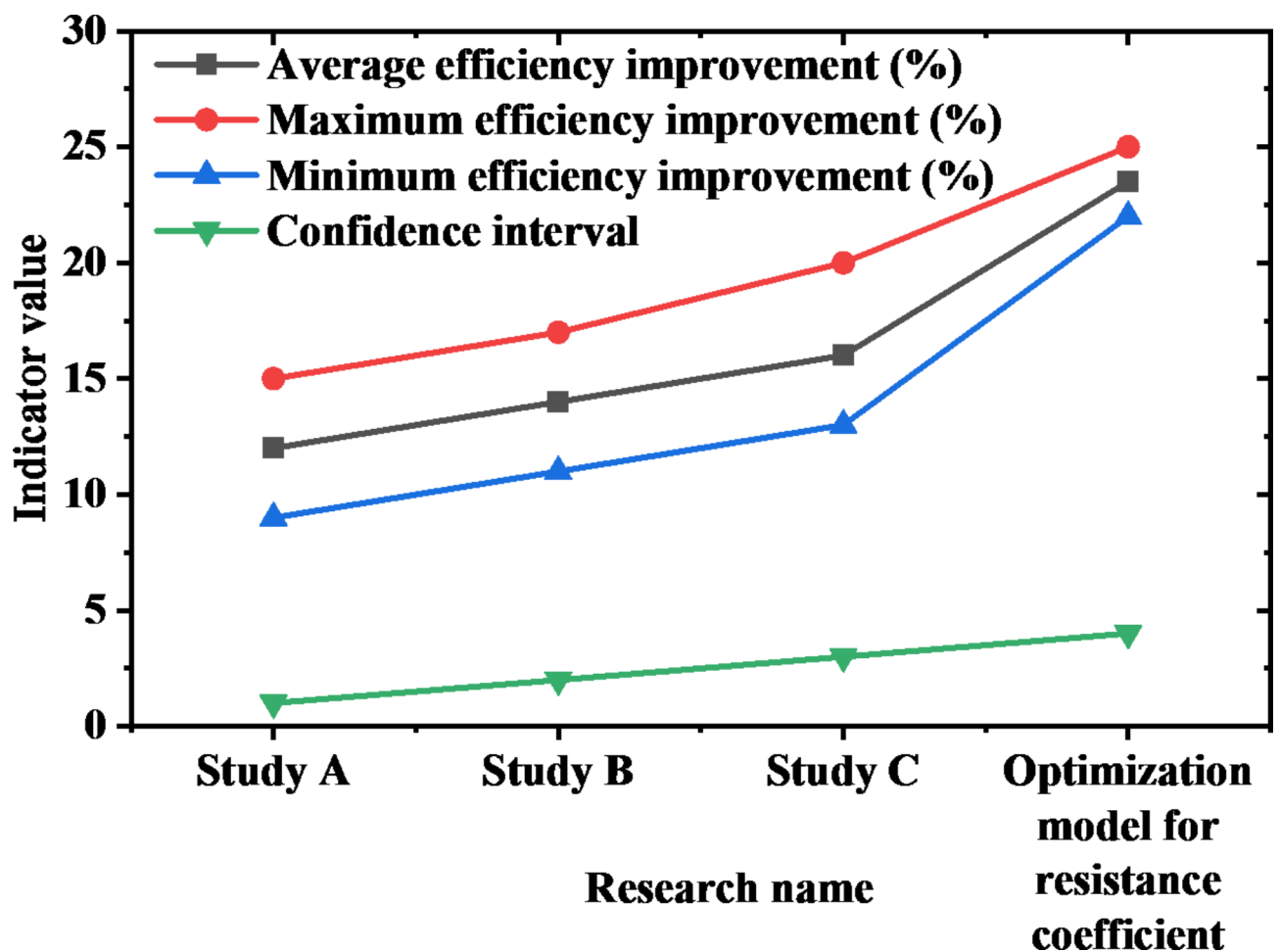


Fig. 9. Comparison and confidence interval of efficiency improvement between similar studies and this study.

through meticulous geometric and structural parameter adjustments. Study C³⁶ centers on innovative control strategies, employing advanced control algorithms to optimize the operation mode of electromagnetic repulsion mechanisms, thereby enhancing their energy conversion efficiency. This study endeavors to enhance overall performance through intelligent and precise control methods from a system control perspective.

Figure 9 compares the efficiency improvement data from different studies, highlighting the superiority of resistance coefficient optimization in this study over similar alternative technological approaches. The average efficiency improvement in this study stands at 23.5%, with a maximum enhancement of 25.0%, while efficiency improvements in similar studies range from 9 to 20%. This comparison not only underscores the methodological superiority of this study but also underscores its substantial practical potential. The narrower confidence interval of $\pm 1.8\%$ reflects the high credibility and precision of the results.

The optimization of the resistance coefficient evidently plays a pivotal role in enhancing the energy conversion efficiency of electromagnetic repulsion mechanisms. The alignment between theoretical simulations and experimental validations underscores the effectiveness and reliability of this optimization strategy. Compared to similar studies, the efficiency improvement demonstrated here is notably higher, emphasizing the considerable advantage of the resistance coefficient optimization model in boosting energy conversion efficiency.

The significance of this study extends beyond its scientific findings, offering practical and viable optimization methods for the design and enhancement of electromagnetic repulsion mechanisms. This optimization not only amplifies energy conversion efficiency but also holds potential for reducing energy losses, thus contributing significantly to energy conservation and system performance enhancement. Moreover, this study equips future researchers and engineers with a robust tool for making more scientifically informed decisions when designing more efficient electromagnetic devices. The state-of-the-art technical solutions discussed in this study have been comprehensively compared in terms of material science, structural design, and control strategies. The drag coefficient optimization method demonstrated exceptional performance across various operational conditions. This success is attributed not only to the effectiveness of the proposed drag coefficient optimization model but also to the integration of experimental verification and numerical simulation.

The optimization of the drag coefficient has proven effective in enhancing energy conversion efficiency, both in theoretical research and practical applications. This optimization strategy offers significant potential across several fields:

- 1) Power Switch Equipment: In high-voltage power switches, the optimized drag coefficient enhances the response speed and operational reliability of the switch, thereby reducing energy loss and extending equipment lifespan. This method improves the energy utilization rate, particularly under conditions of frequent operation.
- 2) Electromagnetic Propulsion Systems: For electromagnetic propulsion technologies, such as those used in spacecraft and UAVs, optimizing the drag coefficient can boost thrust generation efficiency and minimize energy loss. This optimization is particularly valuable for systems that require high miniaturization and efficiency.
- 3) Magnetic Levitation Systems: In maglev systems, optimizing the drag coefficient enhances suspension stability and energy efficiency, reduces power consumption, and improves overall system performance.

Several potential challenges and limitations may arise during the practical application of drag coefficient optimization. Firstly, the optimization, which is based on experimental and simulation results under specific conditions, may require additional debugging and verification in different scenarios to ensure the repeatability of its effects. Secondly, environmental factors such as temperature variations or electromagnetic interference could affect certain parameters in the optimization process, potentially leading to discrepancies between actual performance and theoretical predictions. Additionally, cost considerations must be addressed, particularly for large-scale applications. The impact of the optimized drag coefficient on overall system costs warrants further evaluation.

In summary, while the optimized drag coefficient has demonstrated substantial advantages in theoretical and experimental contexts, practical applications must address issues related to environmental adaptability, cost-effectiveness, and long-term stability. These factors will be the focus of future research to ensure the feasibility and economic viability of the optimization results in real-world scenarios.

Conclusion

Through a comprehensive approach encompassing theoretical analysis, numerical simulation, and experimental validation, this study investigates the influence of the resistance coefficient on the energy conversion efficiency of electromagnetic repulsion mechanisms, leading to a significant performance enhancement. Initially, a mathematical model of the electromagnetic repulsion mechanism is developed through theoretical analysis, followed by sensitivity analysis to elucidate the pivotal role of the resistance coefficient in the energy conversion process. Subsequently, FEA techniques are employed to conduct detailed simulations of electromagnetic repulsion mechanisms under varying resistance coefficients, validating the theoretical analysis. Finally, by constructing an experimental platform and comparing experimental data with simulation results, this study confirms the significance of the resistance coefficient in improving energy conversion efficiency and demonstrates that optimizing it can notably enhance the performance of electromagnetic repulsion mechanisms.

The principal contribution of this study is the significant enhancement of the drag coefficient for improving energy conversion efficiency through a systematic optimization strategy. This achievement not only confirms the accuracy of the theoretical model but also validates the effectiveness of the optimization method with experimental data. The findings reveal that, despite the complex and variable nature of the operating environment of the electromagnetic repulsion mechanism, environmental factors such as temperature and humidity can influence the drag coefficient and, consequently, the energy conversion efficiency. Future research should address these environmental effects and seek to develop more robust optimization strategies. Furthermore, the study demonstrates the potential benefits of integrating intelligent control algorithms with drag coefficient adjustment, offering new avenues for optimizing the dynamic response and operational efficiency of the electromagnetic

repulsion mechanism. This research presents novel perspectives and methodologies for enhancing the performance of the electromagnetic repulsion mechanism, emphasizes the importance of optimizing energy conversion efficiency under complex conditions, and outlines directions for future research. By providing a comprehensive analysis of the drag coefficient and control strategies, this study establishes a foundation for advancing the application performance of the electromagnetic repulsion mechanism and offers a valuable reference for related research.

Data availability

All data generated or analysed during this study are included in this published article (and its Supplementary Information files).

Received: 8 May 2024; Accepted: 27 September 2024

Published online: 30 October 2024

References

1. Yan, B., Yu, N. & Wu, C. A state-of-the-art review on low-frequency nonlinear vibration isolation with electromagnetic mechanisms[J]. *Appl. Math. Mech.* **43** (7), 1045–1062 (2022).
2. Li, S. et al. High solid-solution strengthening mechanism of a novel aluminum-lithium alloy fabricated by electromagnetic near-net shape technology[J]. *Mater. Sci. Engineering: A*. **829**, 142148 (2022).
3. Hao, D. et al. An electromagnetic energy harvester with a half-wave rectification mechanism for military personnel[J]. *Sustain. Energy Technol. Assess.* **57**, 103184 (2023).
4. Xu, J. et al. Modeling and performance evaluation of a bi-stable electromagnetic energy harvester with tri-magnet levitation structure[J]. *Sens. Actuators A: Phys.* **346**, 113828 (2022).
5. Wang, Y. et al. An electromagnetic vibration energy harvester using a magnet-array-based vibration-to-rotation conversion mechanism[J]. *Energy. Conv. Manag.* **253**, 115146 (2022).
6. Bai, S. et al. Electromagnetic-triboelectric energy harvester based on vibration-to-rotation conversion for human motion energy exploitation[J]. *Appl. Energy*. **329**, 120292 (2023).
7. Qu, M. et al. An improved electromagnetism-like mechanism algorithm for energy-aware many-objective flexible job shop scheduling[J]. *Int. J. Adv. Manuf. Technol.* **119** (7), 4265–4275 (2022).
8. Shahzad, F. et al. Electromagnetic control and dynamics of generalized burgers' nanoliquid flow containing motile microorganisms with Cattaneo–Christov relations: Galerkin finite element mechanism[J]. *Appl. Sci.* **12** (17), 8636 (2022).
9. Zhou, J. et al. Design and research of hybrid piezoelectric-electromagnetic energy harvester based on magnetic couple suction-repulsion motion and centrifugal action[J]. *Energy. Conv. Manag.* **258**, 115504 (2022).
10. Zheng, X. et al. A review of piezoelectric energy harvesters for harvesting wind energy[J]. *Sens. Actuators A: Phys.* **352**, 114190 (2023).
11. Zhang, J., Xing, Y. & Pang, H. Research on the mechanism of electromagnetic ultrasonic energy transfer based on dynamic multi-magnetic vector coupling[J]. *Meas. Sci. Technol.* **35** (2), 025109 (2023).
12. Vidal, J. V. et al. Hybrid triboelectric-electromagnetic nanogenerators for mechanical energy harvesting: a review[J]. *Nano-Micro Lett.* **13**, 1–58 (2021).
13. Liu, Z. et al. A new concept of speed amplified nonlinear electromagnetic vibration energy harvester through fixed pulley wheel mechanisms and magnetic springs[J]. *Mech. Syst. Signal Process.* **126**, 305–325 (2019).
14. He, L. et al. A rotating piezoelectric-electromagnetic hybrid harvester for water flow energy[J]. *Energy. Conv. Manag.* **290**, 117221 (2023).
15. Chen, Q., Li, C. & Lv, M. An array magnetic coupling piezoelectric and electromagnetic energy harvester for rotary excitation[J]. *Micromachines*. **14** (8), 1527 (2023).
16. Fang, J. et al. A piezoelectric–electromagnetic hybrid energy harvester inspired by flapping motion of the Diptera insect[J]. *Smart Mater. Struct.* **32** (10), 105018 (2023).
17. Ruan, J. et al. Study on adaptive excitation system of transmission line galloping based on electromagnetic repulsive mechanism[J]. *Shock and Vibration*, 2021: 1–18. (2021).
18. Gao, M. et al. Experimental investigation of non-linear multi-stable electromagnetic-induction energy harvesting mechanism by magnetic levitation oscillation[J]. *Appl. Energy*. **220**, 856–875 (2018).
19. Zhuo, J. et al. Plucking and linear-to-rotary hybrid harvester for low-amplitude vibrations of high-speed railway with an innovative three-step amplification mechanism[J]. *Appl. Energy*. **347**, 121363 (2023).
20. Yao, W. et al. The transformation mechanisms of vortex structures on vortex-induced vibration of an elastically mounted sphere by Lorentz force[J]. *Ocean Eng.* **280**, 114436 (2023).
21. Wang, X. et al. An omnidirectional hybrid wind-wave energy harvester based on a coaxial contra-rotation mechanism for unmanned surface vessels[J]. *Energy. Conv. Manag.* **293**, 117517 (2023).
22. Cao, M. S. et al. Electromagnetic response and energy conversion for functions and devices in low-dimensional materials[J]. *Adv. Funct. Mater.* **29** (25), 1807398 (2019).
23. Sun, R., Zhou, S. & Cheng, L. Ultra-low frequency vibration energy harvesting: mechanisms, enhancement techniques, and scaling laws[J]. *Energy. Conv. Manag.* **276**, 116585 (2023).
24. Lv, H. et al. Electromagnetic absorption materials: current progress and new frontiers[J]. *Prog. Mater. Sci.* **127**, 100946 (2022).
25. Wang, C. et al. A speed-amplified tri-stable piezoelectric-electromagnetic-triboelectric hybrid energy harvester for low-frequency applications[J]. *Nano Energy*. **114**, 108630 (2023).
26. Liu, F. et al. Mechanism investigation for the influence of laser power on droplet transfer behaviors in laser-MIG hybrid welding[J]. *Opt. Laser Technol.* **157**, 108750 (2023).
27. Ding, C. et al. Structural optimization design of electromagnetic repulsion mechanism based on BP Neural Network and NSGA-II[J]. *IEEE Trans. Electr. Electron. Eng.* **18** (12), 1914–1922 (2023).
28. Li, Z. et al. Effects of rolling motion on flow and heat transfer characteristics in a tube bundle channel[J]. *Appl. Therm. Eng.* **220**, 119696 (2023).
29. Ahmad, M. M., Khan, N. M. & Khan, F. U. Review of frequency up-conversion vibration energy harvesters using impact and plucking mechanism[J]. *Int. J. Energy Res.* **45** (11), 15609–15645 (2021).
30. Halim, M. A. & Park, J. Y. Modeling and experiment of a handy motion driven, frequency up-converting electromagnetic energy harvester using transverse impact by spherical ball[J]. *Sens. Actuators A: Phys.* **229**, 50–58 (2015).
31. Shu, J. C. et al. Molecular patching engineering to drive energy conversion as efficient and environment-friendly cell toward wireless power transmission[J]. *Adv. Funct. Mater.* **30** (10), 1908299 (2020).
32. Li, Y. et al. Efficiency analysis and optimization control for input-parallel output-series wireless power transfer systems[J]. *IEEE Trans. Power Electron.* **35** (1), 1074–1085 (2019).

33. Yin, Y. et al. Analysis and optimization of energy loss reduction in a modified tee with deflectors via energy dissipation and vortex strength[J]. *Energy Build.* **290**, 113094 (2023).
34. Zhao, Y. et al. A novel strategy in electromagnetic wave absorbing and shielding materials design: multi-responsive field effect[J]. *Small Sci.* **2** (2), 2100077 (2022).
35. Wu, Z. et al. Dimensional design and core-shell engineering of nanomaterials for electromagnetic wave absorption[J]. *Adv. Mater.* **34** (11), 2107538 (2022).
36. Huang, X. & Yang, B. Towards novel energy shunt inspired vibration suppression techniques: principles, designs and applications[J]. *Mech. Syst. Signal Process.* **182**, 109496 (2023).

Author contributions

P.Y. and G.L. made substantial contributions to the conception or design of the work. They wrote the main manuscript, collected the related material, designed the model and revised the manuscript critically. Q. prepared all of the figures, drafted the work and conducted data acquisition, analysis, and interpretation. P.Y. is the corresponding author and received the funding. All authors approved the version to be published and agreed to be accountable for all aspects of the work in ensuring that questions related to the accuracy or integrity of any part of the work are appropriately investigated and resolved.

Funding

This work is supported by State Grid Company Limited headquarters management science and technology project “HVDC circuit breaker combination breaking key technology and prototype development” (5500-202220110A-1-1-ZN).

Declarations

Competing interests

The authors declare no competing interests.

Additional information

Correspondence and requests for materials should be addressed to P.C.

Reprints and permissions information is available at www.nature.com/reprints.

Publisher's note Springer Nature remains neutral with regard to jurisdictional claims in published maps and institutional affiliations.

Open Access This article is licensed under a Creative Commons Attribution-NonCommercial-NoDerivatives 4.0 International License, which permits any non-commercial use, sharing, distribution and reproduction in any medium or format, as long as you give appropriate credit to the original author(s) and the source, provide a link to the Creative Commons licence, and indicate if you modified the licensed material. You do not have permission under this licence to share adapted material derived from this article or parts of it. The images or other third party material in this article are included in the article's Creative Commons licence, unless indicated otherwise in a credit line to the material. If material is not included in the article's Creative Commons licence and your intended use is not permitted by statutory regulation or exceeds the permitted use, you will need to obtain permission directly from the copyright holder. To view a copy of this licence, visit <http://creativecommons.org/licenses/by-nc-nd/4.0/>.

© The Author(s) 2024